SUPPLEMENTAL MATERIAL

Role of apolipoprotein A-II in the structure and remodeling of human high-density lipoprotein

Xuan Gao, Shujun Yuan, Shobini Jayaraman, Olga Gursky.

MATERIALS AND METHODS

Isolation of human HDL fractions and enrichment with apoA-II

Single-donor HDL from plasma of four healthy volunteers were used. Fresh EDTA-treated plasma was obtained from the blood bank according to the rules of the institutional review board and with donors' written consent. Total HDL were isolated by density gradient ultracentrifugation in the density range 1.063-1.21 g·mL^{-1} [1] and were dialyzed against standard buffer (10 mM Na phosphate, 1 mM EDTA, pH 7.5) for further studies. Size-exclusion chromatography (SEC) was used to isolate HDL fractions homogeneous in size. Total HDL (20 mg/mL protein) was applied to a Superdex 200 XK 16/100 column on an ÄKTA FPLC system (GE Healthcare), the samples were run at a flow rate 0.8 mL/min in standard buffer,and HDL elution was monitored by UV absorbance at 280 nm. The eluted HDL were collected in five 4 mL fractions, 1 to 5 (shortest to longest elution time) and used for further studies. In addition, plasma HDL were isolated into five-to-seven fractions by density gradient centrifugation. The results obtained from the density and the size fractions of HDL were in good agreement. Protein concentration was determined by a modified Lowry assay. Total HDL and their fractions were stored at 4 ^{o}C and were used within 3 weeks. All experiments were repeated 3 or more times. The results reported here were reproducible for all HDL batches explored.

ApoA-I and apoA-II were isolated from human HDL as described [2]. Briefly, HDL were incubated with 6 M Gdn HCl at 37 ^{o}C for 3 h to produce a mixture of dissociated apoA-I and apoA-I-depleted HDL. This mixture was dialyzed against the standard buffer, adjusted to 1.21 g/mL density with KBr, and spun for 40 h at 10 ^{o}C, 50,000 rpm using Ti50.2 rotor. The bottom third contained apoA-I. The top fraction that contained apoA-I-depleted HDL was dialyzed, lyophilized, and delipidated to produce a mixture of apoA-I, apoA-II and apoCs. This mixture was dissolved in 10 mM Tris HCl, 6M Urea, pH 8.0 and applied to a Tricon Mono Q 5/50 GL column (GE Healthcare). The protein was eluted in 10 mM Tris HCl, 6 M Urea with a linear gradient of 0-0.2 M NaCl. The fractions containing apoA-II were pooled and dialyzed against the standard buffer. ApoA-II dimer migrated as a single band on 15% SDS PAGE. Matrix-assisted laser desorption/ionization time-of-flight (MALDI-TOF) analysis of the purified apoA-II confirmed its molecular weight of 17.4 kDa (data not shown). ApoA-II obtained by this method is folded and functional, as indicated by far-UV circular dichroism (CD) spectra (data not shown) and by the ability to form discoidal reconstituted HDL [3].

To obtain HDL enriched with human apoA-II, total plasma HDL and their isolated fractions were incubated at 22 ^{o}C overnight with apoA-II$_{dimer}$ using 1:1 to 3:1 weight ratios of excess apoA-II to total HDL protein. HDL co-incubated with human apoA-I under otherwise identical conditions were used as controls. After incubation, HDL were re-isolated from the uncomplexed protein by SEC using Superdex 200 10/300 GL column, and were used for further studies.

HDL characterization

Particle size was assessed by non-denaturing gel electrophoresis (NDGE) and electron microscopy (EM). For NDGE, lipoprotein samples containing 10 μg protein were run on 8% gels at 120 V for ~2 h. The gels were stained with Denville protein stain. Negative stain EM was performed at 22 ^{o}C by using a CM12 transmission electron microscope (Philips Electron Optics) as described [4].

SEC was used to separate and characterize HDL fractions before and after incubation with apoA-II. The samples were run on a Superdex 200 10/300 GL column (GE Biosciences) at a flow rate of 0.5 mL/min in standard buffer. The protein size was assessed from the calibration plot by using molecular-size markers (Bio-Rad). Protein composition in SEC peak fractions was determined by using 15% SDS PAGE. Image J software was used to calculate the band intensities in SDS PAGE (Rasband W.S., Image J, http://rsb.info.nih.gov/ij/). Such analysis helps compare apoA-I:apoA-II ratios on various HDL but has limited accuracy, in part, because of the staining artifacts inherent to apoA-II [5].

MALDI-TOF MS was used to assess protein composition in HDL fractions using Reflex-IV instrument (Bruker Daltonics) as described [6]. HDL samples (1 mg/mL protein in standard buffer) were mixed with equal volume of the matrix. The instrument was calibrated in linear mode. The spectra were collected as an average of 100 laser shots at a power varying from 50-80%. Multiple spectra in the range corresponding to 3-200 kDa were collected from the same sample covering the entire sample area.

An AVIV-400 CD spectrometer with a thermoelectric temperature controller was used to monitor protein secondary structure and HDL thermal denaturation. The fluorescence accessory was used to monitor right-angle light scattering that reports on the increase in the particle size upon heat-induced lipoprotein fusion and rupture [6]. HDL samples (0.02 mg/mL protein in standard buffer containing 150 mM NaCl, placed in a 5 mm path length cell) were heated and cooled from 10 to 98 ^{o}C at a constant rate of 6 ^{o}C/h. Thermal denaturation of HDL was monitored at 222 nm by light scattering for particle fusion and rupture, and by CD for α-helical unfolding. The melting data recorded by CD (not shown) and light scattering closely correlated and showed similar trends.

RESULTS

Distribution of endogenous apoA-II in fractions of human HDL isolated by size or density

Human plasma HDL were separated by SEC into five fractions (Fig. S1A), from 1 (large) to 5 (small). Each fraction was assessed for particle size by NDGE and EM (Fig. S1B, S2) and for protein composition by SDS PAGE and MALDI-TOF MS (Fig. S1C, D). In addition to the major protein, apoA-I, HDL fractions 3-5 contained apoA-II as their second-major protein; all fractions also contained minor HDL proteins, apoCs (Fig. S1C, D). Thus, in contrast to apoA-I and apoCs, apoA-II was found mainly on the mid-size plasma HDL (fractions 3, 4); no apoA-II was found on the large HDL (fractions 1, 2). Despite batch-to-batch variations in the exact amount of apoA-II in total HDL and its individual fractions, the medium HDL fractions always contained the vast majority of apoA-II, the smallest and densest HDL isolated by density or size into 5 or more fractions contained little if any apoA-II, and the large buoyant HDL contained no apoA-II (Figs. S1, S2). This agrees with other studies, including MS analysis of human HDL(A-I) and HDL(A-I/A-II) fractions isolated by immunoaffinity and SEC, which detected apoA-II only in the mid-size particles [8, 9].

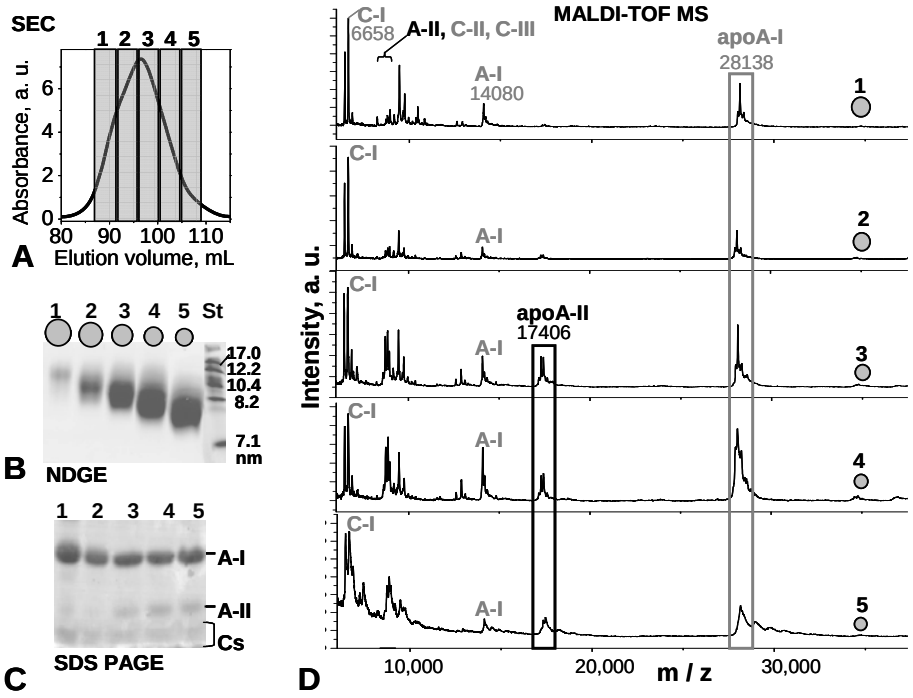

Figure S1. Particle size and protein composition in size fractions of human HDL. Fractions 1-5 were isolated by SEC from single-donor HDL (**A**). Particle size was assessed by NDGE (**B**). Protein composition was assessed by 15% SDS PAGE, Coomassie blue stain (**C**) and by MALDI-TOF MS (**D**). Boxes show characteristic peaks of apoA-I and apoA-II. Peak positions for apoC-I, apoC-II, apoC-III, and the double-ionized form of apoA-I (~14.1 kDa) and apoA-II (8,7 kDa) are indicated.

Figure S2. Electron microscopic analysis of negatively stained size fractions of human HDL. Fractions 1-5 were isolated by SEC from single-donor plasma HDL (see Fig. S1A). The particle diameters (tabulated) were assessed from these micrographs using ~200 particles per frame. Standard error of mean (SEM) reflects the accuracy in the determination of the mean diameter <d>; standard deviation (STD) reflects heterogeneity in the particle diameter. The results for total HDL are shown for comparison. These results are in good agreement with NDGE analysis of HDL size fractions (Fig. S1B).

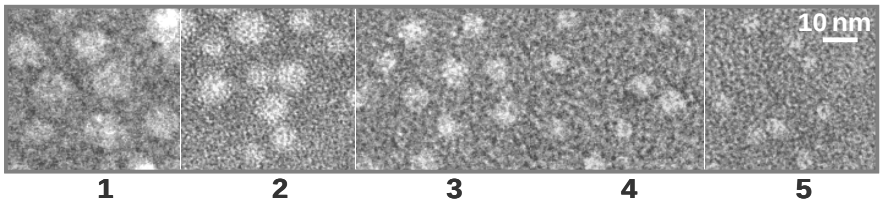

	HDL Size Fraction					Total HDL
Native HDL	**1**	**2**	**3**	**4**	**5**	
<d>, nm	11.6	10.7	9.4	8.5	7.5	9.9
SEM, nm	0.09	0.11	0.08	0.09	0.08	0.13
STD, nm	1.1	1.1	0.9	0.9	0.9	1.7

Figure S3. Particle size and protein composition in density fractions of human plasma HDL. Single-donor total human HDL (density range 1.06-1.21 g/ml) were isolated by gradient density centrifugation into five fractions with mean density of 1.0730 (I), 1.1018 (II), 1.1375 (III), 1.1544 (IV), or 1.1939 g/ml (V) Each fraction was assessed by SDS PAGE for protein composition and by NDGE for particle size. Data for total HDL and for lipid-free apoA-I are shown for comparison. The results are in good agreement with those of HDL size fractions (Fig. S1) and show that endogenous apoA-II circulates mainly to the mid-size human HDL.

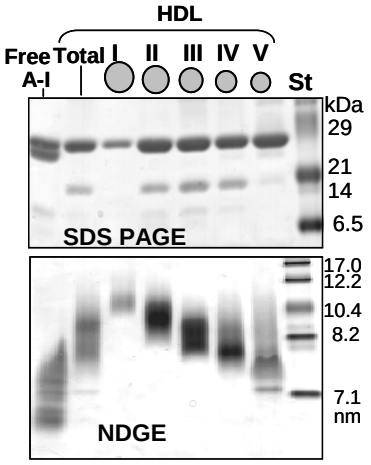

Effects of binding of exogenous apoA-II on the size and composition of human HDL

To assess the effects of exogenous apoA-II on the structure and stability of size fractions of human HDL, each fraction was incubated with human apoA-II using 1:1 weight ratio of excess apoA-II to total HDL protein. Our results show that under these conditions, apoA-II displaces some but not all apoA-I from HDL, consistent with the earlier studies of reconstituted HDL [10, 11]. SEC data of the incubation mixture clearly resolved lipoprotein from the proteins in solution (peaks 1 and 2 in Fig. S4A). SDS PAGE showed that peak 1 contained HDL enriched with apoA-II, while peak 2 contained mainly apoA-I displaced from HDL (Fig. S4A, B). SDS PAGE also showed that nearly all exogenous

apoA-II was anchored to HDL, while a substantial portion of apoA-I was displaced (Fig. S4B). Analysis of the band intensities in SDS PAGE of the apoA-II-enriched HDL suggested that the apoA-II:apoA-I intensity ratio increased from ~1:3 in intact HDL to 3:2 in HDL(A-I+A-II). Staining artifacts inherent to apoA-II [5] prevented accurate stoichiometric analysis of these particles based on SDS PAGE.

SEC data of the total human plasma HDL showed that HDL enrichment with exogenous apoA-II led to a small but consistent shift in peak 1 towards higher volumes (Fig. S4D). Similarly, individual HDL size fractions showed small shifts in peak 1 to higher volumes (slightly larger particles) but no detectable changes in the peak width upon enrichment with apoA-II (Fig. S4C). This result, confirmed by NDGE (not shown), is consistent with the earlier studies [12-14] and reflects an increase in the hydrodynamic radius of HDL upon binding of additional protein. In summary, although apoA-II circulates mainly on the mid-size plasma HDL, exogenous apoA-II can bind to HDL of any size and thereby slightly increase this size but cause no large changes in the particle size distribution.

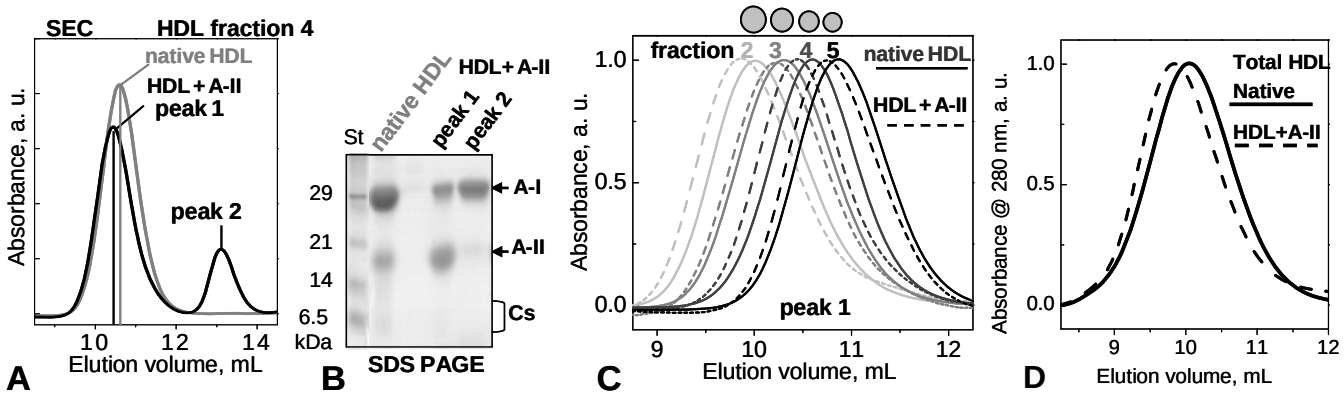

Figure S4. Protein composition in HDL after incubation with human apoA-II using 1:1 weight ratio of exogenous apoA-II to total HDL protein. (**A**) SEC of human HDL before (grey) and after incubation with apoA-II (black). Representative data for HDL fraction 4 are shown; similar SEC profiles were observed in other fractions. Two protein-containing peaks in the incubation mixture are marked 1 and 2. (**B**) SDS PAGE of the SEC peak fractions corresponding to native HDL (grey) and to peaks 1 and 2 isolated from HDL that have been incubated with apoA-II (black). Peak 1 is apoA-II-enriched HDL (marked HDL+A-II) and peak 2 is protein in solution. St - molecular weight standards. (**C**) SEC data of peak 1 in HDL fractions 1-5 before (solid lines) and after (dashed lines) incubation with apoA-II; (**D**) similar data for total plasma HDL.

Effects of exogenous apoA-II on structural stability of human HDL

Thermal denaturation was used to test the effects of apoA-II enrichment on the structural stability of size fractions of human HDL. Earlier, we showed that thermal stability of human HDL correlates inversely with the particle diameter [4]. The effect of apoA-II in these studies was unclear, in part, because apoA-II comprises only about 20% of the total protein in human HDL [15-18]. In an attempt to amplify the effect of apoA-II on HDL stability, HDL fractions 1-5 were incubated with apoA-II using 1:1 weight ratio of excess apoA-II to total HDL protein. Such incubation causes no significant changes in HDL lipid composition [10] but increases the apoA-II : apoA-I ratio on HDL (Fig. S4). The apoA-II-enriched HDL were isolated by SEC (peak 1, Fig. S4A) and were subjected to thermal denaturation to assess lipoprotein stability.

The heating of plasma HDL induces apolipoprotein dissociation and lipoprotein fusion and rupture ([19] and references therein). Figure S5 shows representative melting data recorded from HDL fractions 1 and 4 before (grey) and after their enrichment with apoA-II (black). These and other melting data clearly show that the enrichment of any HDL fraction with apoA-II increases the apparent transition temperature, $T_{m,app}$, by 12-15 ^{o}C (Fig. S5). In contrast, HDL that have been incubated with excess apoA-I under otherwise identical conditions showed little if any change in $T_{m,app}$ (not shown). We conclude that enrichment with exogenous apoA-II greatly stabilizes plasma spherical HDL.

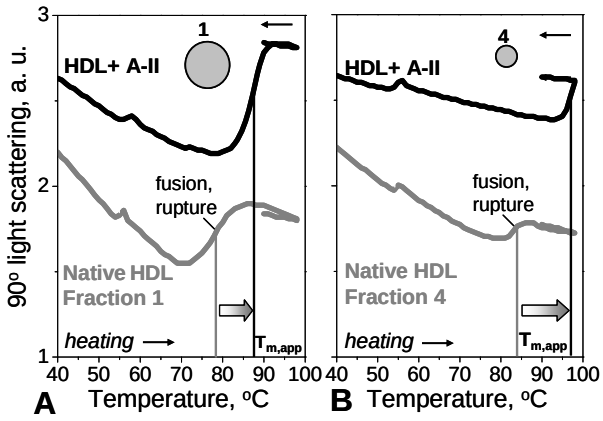

Figure S5. Effect of enrichment with apoA-II on the thermal stability of HDL fractions. HDL were either native (grey) or incubated with apoA-II using 1:1 weight ratio of exogenous apoA-I to total HDL protein, followed by removal of uncomplexed protein by SEC (black). The resulting apoA-II-enriched HDL (HDL+A-II) correspond to peak I in Figure S4A. Representative melting data recorded from HDL fractions 1 and 4 are shown; similar trends were observed in other fractions. The samples (0.02 mg/mL protein and 150 mM NaCl in standard buffer) were heated and cooled at a rate of 6 ^{o}C/h. Heat-induced increase in the particle size due to fusion and rupture was monitored by right-angle light scattering using the fluorimeter attachment in the AVIV-400 CD spectropolarimeter (former 315 model). An optical artifact of the instrument contributed to the negative slope in the heating data [7]. Vertical lines indicate the apparent transition temperature $T_{m,app}$. The large arrow indicates changes in $T_{m,app}$ upon HDL enrichment with apoA-II. Thin arrows show directions of temperature changes.

Spherical HDL(A-II) obtained by enrichment of human HDL

ApoA-II was proposed to form specific stabilizing interactions with apoA-I on the surface of spherical rHDL [12]. To probe whether such interactions can account for the increased stability of human spherical HDL enriched with exogenous apoA-II (Fig. S5), we tested whether this increased stability is also characteristic of HDL(A-II). Plasma HDL were incubated with apoA-II using 3:1 weight ratio of excess apoA-II to total HDL protein. Under these conditions, apoA-I was completely displaced by apoA-II from HDL, consistent with the earlier studies of rHDL [11]. This is illustrated by SDS PAGE showing that the resulting particles, HDL(A-II), contained apoA-II but essentially no apoA-I (Fig. S6A). Compared with their native progenitors, spherical HDL(A-II) showed slightly lower electrophoretic mobility but similar band width on NDGE (Fig. S6B), suggesting that additional protein bound at their surface caused no large changes in the particle diameter. EM analysis was consistent with this interpretation and showed no large differences in the particle diameter distribution of native HDL and HDL(A-II) not shown). Furthermore, CD and light scattering melting data clearly showed that HDL(A-II) were much more stable towards rupture than their native HDL progenitors, as evident from an increase in $T_{m,app}$ by >15 ^{o}C (Fig. S6C). Thus, the stabilizing effect of excess apoA-II on the spherical particles is not limited to HDL(A-I/A-II) but extends to HDL(A-II). Consequently, this effect cannot be accounted for by the stabilizing interactions between apoA-II and apoA-I, and must result from the inherent properties of apoA-II, such as its high hydrophobicity (Fig. S7 below).

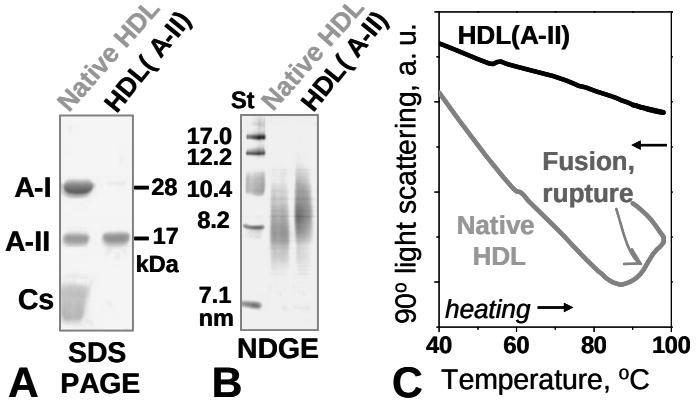

Figure S6. Characterization of spherical HDL(A-II) containing apoA-II but no apoA-I. Human plasma HDL were incubated with apoA-II using 3:1 weight ratio of excess apoA-II to total HDL protein, leading to complete displacement of apoA-I. The resulting HDL(A-II) that were re-isolated by SEC (black) and their native progenitors (grey) were analyzed by SDS PAGE for protein composition (**A**), by NDGE for particle size (**B**), and by right-angle light scattering for thermal stability (**C**). Molecular weights corresponding to apoA-I and apoA-II_{dimer} are indicated in panel A. The melting data in panel C were recorded as described in Figure S5. Under these conditions, this batch of native HDL showed heat-induced fusion and rupture above 85 ^{o}C (gray line). In contrast, fusion and rupture of HDL(A-II) were not detected in the temperature range below 98 ^{o}C and hence, were shifted above 98 ^{o}C, indicating increased stability of HDL(A-II) compared to their native progenitors.

Evidence for the apoA-II-induced contraction of apoA-I on HDL surface

Contraction of apoA-I on HDL surface induced by binding of apoA-II is supported by the recent studies of mid-size discoidal rHDL(A-I/A-II) (d~9.6 nm) containing two copies of apoA-I and one copy of apoA-II_{dimer}, obtained by enrichment of mid-size discoidal rHDL(A-I) with apoA-II [20]. On the basis of H/D exchange and Lys modification studies, Silva's team reported that such enrichment induces limited conformational changes in apoA-I leading to increased exposure of repeats 8-9 and reduced exposure of repeat 4 [20]. Our model explains this observation by the contraction of the apoA-I variable region, from the mid-size conformation with a 3-segment buckle to a more compact 4-segment buckle (Fig. 2). This contraction increases the exposure of the C-terminal repeats 8-9 but reduces the exposure of repeat 4 in apoA-I (Fig. 2A and C compared), in excellent agreement with Silva's results. Furthermore, Silva's team proposed that, in mid-size discoidal rHDL(A-I/A-II), apoA-I double-belt is wrapped around the disk perimeter while apoA-II_{dimer} is located across the top or the bottom of the particle in a separate plane [20]. This is consistent with our model of mid-size spherical HDL(A-I/A-II) (Fig. 2C) and suggests that HDL disks and spheres of similar diameters and protein composition may have similar protein arrangement on their surface. This explains why apoA-II helps form homogeneous mid-size spherical HDL(A-I/A-II) In summary, the conformational ensemble depicted in Figure 2 helps explain why apoA-II is found in circulation mainly on the mid-size human HDL, and suggests specific conformational changes in apoA-I that can be induced by binding of apoA-II to HDL surface [10, 11, 20-22].

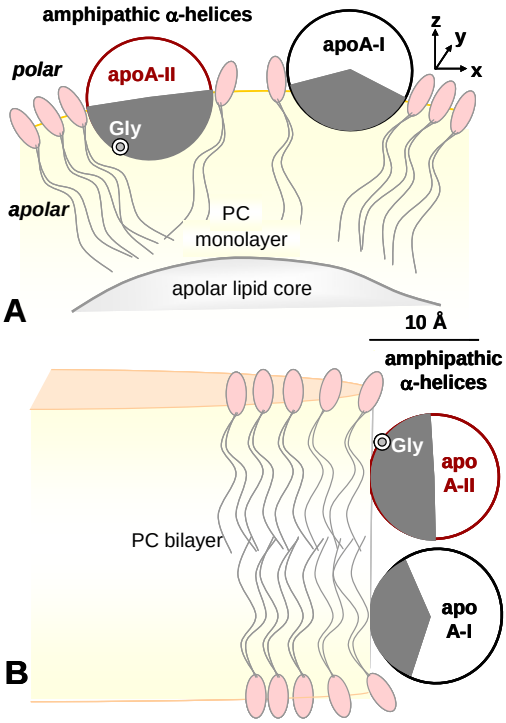

Figure S7. Possible arrangement of the amphipathic apolipo-protein α-helices of apoA-I and apoA-II on the surface of HDL disks and spheres. The class-A α-helices running along the Y-axis are shown in a cross-section by circles. Apolar helical faces are filled in gray. The helices are shown at the top of phosphotidyl-choline (PC) monolayer on the surface of spherical HDL (A) or around the perimeter of a PC bilayer in discoidal HDL (B). Positions of G22 and G57 in apoA-II are indicated by 'Gly'. We speculate that helical kinks at these Gly can induce overall molecular curvature along the helical axis (Fig. 1). The kinked helices running along the Y-axis can confer lipid curvature in Y-direction. Panel A illustrates that helical insertion on the top of the phospholipid monolayer helps confer monolayer curvature in the X-direction: the deeper the insertion the larger the curvature.

REFERENCES CITED

[1] Schumaker, V. N., and Puppione, D. L. 1986. Sequential flotation ultracentrifugation. *Methods Enzymol.* 128, 151-170.

[2] Cheung, M. C., and Albers, J. J. 1984. Characterization of lipoprotein particles isolated by immunoaffinity chromatography. Particles containing A-I and A-II and particles containing A-I but no A-II. *J. Biol. Chem.* 259(19): 12201-122219.

[3] Jayaraman, S., Gantz, D. L., and Gursky, O. 2005. Kinetic stabilization and fusion of apolipoprotein A-2:DMPC disks: comparison with apoA-1 and apoC-1. *Biophys. J*. 88(4): 2907-2918.

[4] Gao, X., Yuan, S., Jayaraman, S. and Gursky, O. 2009. Differential stability of high-density lipoprotein subclasses: effects of particle size and protein composition. *J. Mol. Biol*. 387(3): 628-638.

[5] Gauthamadasa, K., Vaitinadin, N. S., Dressman, J. L., Macha, S., Homan, R., Greis, K. D., and Silva, R. A. 2012. Apolipoprotein A-II mediated conformational changes of apolipoprotein A-I in discoidal high density lipoproteins. *J Biol. Chem.* 287(10), 7615-7625.

[6] Jayaraman, S., Cavigiolio, G., and Gursky, O. 2012. Folded functional lipid-poor apolipoprotein A-I obtained by heating of high-density lipoproteins: Relevance to HDL biogenesis. *Biochem. J*. 442(3): 703-712.

[7] Benjwal, S., Verma, S., Röhm, K. H., and Gursky, O. 2006. Monitoring protein aggregation during thermal unfolding in circular dichroism experiments. *Protein Sci*. 15(3): 635-639.

[8] Gordon, S. M., Deng, J., Lu, L. J., and Davidson, W. S. 2010. Proteomic characterization of human plasma high density lipoprotein fractionated by gel filtration chromatography. *J. Proteome Res*. 9(10): 5239-5249.

[9] Gauthamadasa, K., Rosales, C., Pownall, H. J., Macha, S., Jerome, W. G., Huang, R. and Silva, R. A. 2010. Speciated human high-density lipoprotein protein proximity profiles. *Biochemistry*, 49(50), 10656-10665.

[10] Edelstein, C., Halari, M., and Scanu, A. M. 1982. On the mechanism of the displacement of apolipoprotein A-I by apolipoprotein A-II from the high density lipoprotein surface. Effect of concentration and molecular forms of apolipoprotein A-II. *J. Biol. Chem*. 257(12): 7189-7195.

[11] Durbin, D. M., and Jonas, A. 1997. The effect of apolipoprotein A-II on the structure and function of apolipoprotein A-I in a homogeneous reconstituted high density lipoprotein particle. *J. Biol. Chem.* 272(50): 31333-31339.

[12] Rye, K. A., Wee, K., Curtiss, L. K., Bonnet, D. J., and Barter, P. J. 2003. Apolipoprotein A-II inhibits high density lipoprotein remodeling and lipid-poor apolipoprotein A-I formation. *J. Biol. Chem.* 278(25), 22530-22536.

[13] Lagrost, L., Persegol, L., Lallemant, C., and Gambert, P. 1994. Influence of apolipoprotein composition of high density lipoprotein particles on cholesteryl ester transfer protein activity: particles containing various proportions of apolipoproteins AI and AII. *J. Biol. Chem.* 269, 3189–3197.

[14] Pilon, A., Briand, O., Lestavel, S., Copin, C., Majd, Z., Fruchart, J. C., Castro, G., and Clavey, V. 2000. Apolipoprotein AII enrichment of HDL enhances their affinity for class B type I scavenger receptor but inhibits specific cholesteryl ester uptake. *Arterioscler. Thromb. Vasc. Biol*. 20(4), 1074-1081.

[15] Yetukuri, L., Huopaniemi, I., Koivuniemi, A., Maranghi, M., Hiukka, A., Nygren, H., Kaski, S., Taskinen, M. R., Vattulainen, I., Jauhiainen, M., and Orešič, M. 2011. High density lipoprotein structural changes and drug response in lipidomic profiles following the long-term fenofibrate therapy in the FIELD substudy. *PLoS One*, 6(8): e23589.

[16] Blanco-Vaca, F., Escolà-Gil, J. C., Martín-Campos, J. M., and Julve, J. 2001. Role of apoA-II in lipid metabolism and atherosclerosis: Advances in the study of an enigmatic protein. *J. Lipid Res*. 42(11): 1727-1739.

[17] Tailleux, A., Duriez, P., Fruchart, J. C., and Clavey, V. 2002. Apolipoprotein A-II, HDL metabolism and atherosclerosis. *Atherosclerosis*, 164(1): 1-13.

[18] Kalopissis, A.D., Pastier, D., and Chambaz, J. 2003. Apolipoprotein A-II: beyond genetic associations with lipid disorders and insulin resistance. *Curr. Opin. Lipidol*. 14: 165–172.

[19] Jayaraman, S., Gantz, D. L., and Gursky, O. 2006. Effects of salt on thermal stability of human plasma high-density lipoproteins. *Biochemistry,* 45, 4620-4628.

[20] Gauthamadasa, K., Vaitinadin, N.S., Dressman, J. L,. Macha, S., Homan, R., Greis, K. D., and Silva, R. A. 2012. Apolipoprotein A-II mediated conformational changes of Apolipoprotein A-I in discoidal high density lipoproteins. *J. Biol. Chem.* 287(10): 7615-7625.

[21] Boucher, J., Ramsamy, T. A., Braschi, S., Sahoo, D., Neville, T. A., and Sparks, D. L. 2004. Apolipoprotein A-II regulates HDL stability and affects hepatic lipase association and activity. *J. Lipid Res.* 45(5): 849-858.

[22] Silva, R. A., Schneeweis, L. A., Krishnan, S. C., Zhang, X., Axelsen, P. H., and Davidson, W. S. 2007. The structure of apolipoprotein A-II in discoidal high density lipoproteins. *J. Biol. Chem.* 282(13): 9713-9121.